

# Stochastic Modeling of Extreme Dry Spells in Southeast Iran: Patterns, Trends, and Return Periods

Marzieh Siroosi, Peyman Mahmoudi, Hamid Nazaripour, and Seyed Mahdi Amir Jahanshahi (2025)

*University of Sistan and Baluchestan, Zahedan, Iran*

DOI: <https://doi.org/10.14796/JWMM.C564>

## ABSTRACT

Southeast Iran, an arid and highly vulnerable region, faces significant challenges from recurrent droughts. Understanding the behavior of extreme dry spells is critical for effective water resource management and drought risk assessment. This study provides a comprehensive stochastic analysis of the Longest Annual Dry Spell (LADS) across this region. Daily precipitation data was utilized from eight meteorological stations spanning 38 years (1985–2022). LADS series were extracted using a precipitation threshold of  $\geq 1$  mm/day. Long-term trends in LADS were assessed using Sen's slope estimator and the Mann–Kendall test for statistical significance. To model the probability of extreme events, five probability distributions—Generalized Extreme Value (GEV), Generalized Pareto (GP), Pearson Type III (PE3), three-parameter log-normal (Lnorm3), and generalized logistic (Glogis)—were fitted to the LADS data, with parameters estimated via the robust L-moments method. The best-fit distribution was identified using Kolmogorov–Smirnov, Anderson–Darling, and Chi-squared goodness-of-fit tests. Subsequently, LADS return periods (2, 5, 10, 25, 50, and 100 years) were calculated. Results indicate a generally non-significant increasing trend in LADS duration across the study area. The PE3 distribution emerged as the most suitable model for LADS frequency analysis in Southeast Iran. Notably, spatial variations exist: Zabol station (north) exhibits the highest LADS risk for shorter return periods (e.g., 185 days for  $T = 10$  years), whereas Iranshahr station (center) shows the highest risk for longer return periods (e.g., 372 days for  $T = 100$  years). These findings offer crucial quantitative insights into extreme dry spell hazards, supporting targeted drought preparedness and adaptation strategies in this climate-sensitive region.

---

Siroosi, M., P. Mahmoudi, H. Nazaripour, and S.M.A. Jahanshahi. 2025. "Stochastic Modeling of Extreme Dry Spells in Southeast Iran: Patterns, Trends, and Return Periods." *Journal of Water Management Modeling* 33: C564. <https://doi.org/10.14796/JWMM.C564> [www.chijournal.org](http://www.chijournal.org) ISSN: 2292-6062 © Siroosi et al. 2025



## 1. INTRODUCTION

Today, climate change is recognized as one of the most significant environmental challenges of the 21st century (Ghaemi et al. 2022; Mishra and Singh 2010). According to the Fifth Assessment Report (AR5) of the Intergovernmental Panel on Climate Change (IPCC) in 2014, the average global temperature rose by approximately 0.85°C between 1880 and 2012 (Zarrin et al. 2022). This rise in the planet's average temperature has led to an increase in extreme climatic events across vast regions of the earth (Bonsal et al.; IPCC 2014). Southwest Asia, particularly Iran, has not been immune to these changes, and climate change has resulted in a higher frequency of extreme climatic events such as droughts and floods (Alizadeh-Choobari and Najafi 2018; Bari Abarghouei et al. 2011; Mansouri Daneshvar et al. 2019; Nouri and Homaei 2020). This surge in extreme climatic events, especially the increased frequency of droughts, has positioned Iran as one of the most economically and socially vulnerable countries to climate change (Madani et al. 2016; Mahmoudi et al. 2019).

Drought is the lack of precipitation over a long period, one of the most complex climatic phenomena often associated with long dry days (Wilhite and Pulwarty 2017). Determining a set of suitable and accurate indicators is of particular importance to monitor and evaluate drought. So far, different indicators have been presented to monitor and evaluate droughts, mostly based on meteorological or hydrological variables. These indicators are generally divided into three categories based on the type of droughts measured. Meteorological drought indices measure droughts caused by lack of precipitation; agricultural drought indices quantitatively examine the drought caused by inadequate soil moisture; and hydrological drought indicators measure droughts caused by surface and subsurface water resource reduction (Chanda et al. 2014). Most of the indices of these three categories of droughts are defined on monthly or seasonal time scales (Vicente-Serrano et al. 2010; McKee et al. 1993; McKee et al. 1995), except for the Palmer Drought Intensity Index (PDSI) (Palmer 1965) and the Effective Drought Index (EDI) (Byun and Wilhite 1999). Data analysis, especially precipitation data on monthly or seasonal scales, has many advantages, but at the same time, it also has disadvantages because it cannot show the driest or wettest period during a month or season. For this reason, many researchers have suggested using the length of dry periods to study droughts (Mahmoudi et al. 2021; She et al. 2013; Anagnostopoulou et al. 2003; Martin-Vide and Gomez 1999; Douguedroit 1987; Kutiel 1985).

Using daily precipitation data from 104 meteorological stations in Switzerland, Schmidli and Frei (2005) studied the variability of heavy precipitation and drought conditions based on a wide range of daily and multi-day precipitation indices. Their results indicated a significant increasing trend in the maximum number of consecutive dry days (with a precipitation threshold of less than 1 mm) in the two seasons of spring and autumn for the southern regions of Switzerland. Based on four precipitation thresholds of 0.1, 1, 5, and 10 mm per day, Serra et al. (2006) extracted the number of dry spells, the maximum length of dry spells, and the average length of dry spells on two annual and semi-annual scales for Catalonia (northeast Spain) and analyzed their long-term changes. This research showed that for all the features extracted for dry spells based on 5- and 10-mm thresholds, a significant decreasing trend can be seen for Catalonia. Cindrić et al. (2010) also extracted the average and maximum length of dry spells for 45 meteorological stations in Croatia using four precipitation thresholds of 0.1, 1, 5, and 10 mm per day and analyzed their changes. The research results of these researchers showed that the

average and maximum length of time for two seasons, winter and spring, had an increasing trend, and for the autumn season, there was a decreasing trend. Deni et al. (2010) showed the changing trends of different dry spell characteristics in Peninsular Malaysia during the monsoon seasons. The results of these researchers showed that the total number of dry days, maximum duration, average, and dry days, especially long-term dry days (at least four consecutive dry days), have decreased. But the only characteristic of dry spells that has been increasing is related to short-term dry spells (dry spells of 1 to 3 days).

Studies focusing specifically on dry spell characteristics using daily data in Iran have gained traction more recently. For instance, Rezaei et al. (2021) utilized the Tropical Rainfall Measuring Mission (TRMM) satellite data (1998–2019) to investigate Maximum Consecutive Dry Days (MCDDs) during winter across Iran. They identified the highest MCDD values in the southeast, observed generally increasing trends in winter MCDDs, and uncovered a complex, non-stationary relationship with the El Niño–Southern Oscillation (ENSO), particularly highlighting differing impacts in early versus mid-winter in the south. Their findings underscored the value of satellite data for spatial analysis and the role of teleconnections in seasonal dry spell patterns. In parallel, Mahmoudi et al. (2021) analyzed daily station precipitation data (41 stations, 1989–2018) to probabilistically model the mean length and frequency of short, medium, and long dry spells across Iran. They confirmed the occurrence of longer dry spells in southern latitudes, reporting an annual maximum dry spell length reaching 351 days in Southeast Iran. A key finding was that while probabilistic models (Exponential, Negative Binomial) adequately simulated the frequency of dry spells, they struggled to accurately reproduce the mean length, especially for spells exceeding 10 days. Earlier work by Mahmoudi et al. (2013), focusing on regionalization based on dry spell lengths (using data from 1981–2004), also concluded that Southeast Iran exhibits significantly higher average and maximum dry spell lengths compared to other regions. Furthermore, Balouchi et al. (2022) confirmed the unique drought conditions in Southeast Iran, noting average drought durations exceeding two years, significantly longer than most other parts of the country. These studies collectively highlight Southeast Iran as a region particularly prone to prolonged dry periods (Mahmoudi et al. 2022).

While the aforementioned studies (Rezaei et al. 2021; Mahmoudi et al. 2021) provide crucial insights into general dry spell patterns, seasonal variations, frequencies, and modeling challenges using daily data across Iran, a dedicated investigation into the extreme facet of dry spells — specifically the Longest Annual Dry Spell (LADS) — and its associated recurrence risk remains less developed, particularly for the vulnerable Southeast region. LADS represents a critical threshold of prolonged water deficit impacting various sectors. Although Mahmoudi et al. (2021) noted challenges in modeling mean spell length, the probabilistic behavior of the LADS warrants specific focus. Methodologies for applying probability distribution functions (PDFs) to hydroclimatic extremes for estimating return periods are well-established in the literature (She et al. 2013; Coles 2001). However, the application of these methods to characterize the risk associated with LADS using long-term daily station records specifically in Southeast Iran—a region consistently identified as highly susceptible to extended dryness—constitutes the primary contribution of this research. Therefore, this study aims to:

1. Characterize the spatial patterns and temporal trends of the LADS in Southeast Iran using daily station precipitation data from 1985–2022, and

- Apply appropriate stochastic modeling techniques, informed by goodness-of-fit tests, to estimate the return periods of these extreme dry spell events.

The results are expected to provide valuable, actionable information for regional water resource planning and drought risk management in this critical area.

## 2. STUDY AREA

The area studied in this research includes the three provinces of Sistan and Baluchestan, Kerman, and Hormozgan in Southeast Iran, which occupies an area of about 433,208 km<sup>2</sup>, equal to 26% of Iran's area (Figure 1a). According to the 2016 census, these three provinces had a population of 7,716,147 people, equal to 9.6% of the total population of Iran (Statistical Center of Iran 2016).

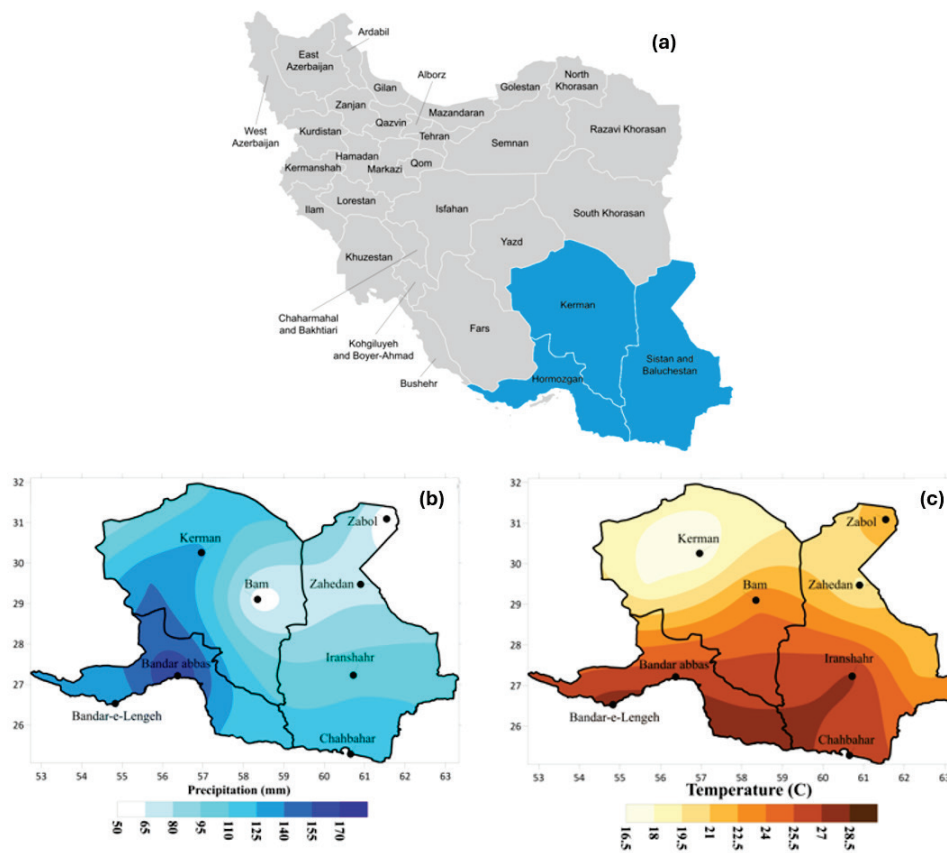


Figure 1 (a) Location of the study area in Southeast Iran, including the three provinces of Sistan and Baluchestan, Kerman and Hormozgan; (b) Spatial distribution of average annual precipitation; and (c) Spatial distribution of average annual temperature.

De Martonne's climatic classification (De Marton 1909) shows that the studied area has a dry climate (Table 1). The average annual precipitation across the study area is approximately 107.8 mm (based on the 1985–2022 data from the eight stations). However, the precipitation regime is characterized by extremely high inter-annual variability, as indicated by a regional Coefficient of Variation (CV) of 42.53%. This high variability, coupled with the low average rainfall, underscores the region's inherent susceptibility to drought conditions, although the spatial distribution of mean precipitation varies significantly across individual stations (Figure

1b). The average annual temperature in this area is 23.8°C. The lowest average annual temperature belongs to Kerman station at 16.9°C, and the highest, at 27.8°C belongs to Bandar Lange station (Figure 1c).

The precipitation regime in Southeast Iran is characterized by a marked seasonality, typical of its arid to hyper-arid climate. The primary rainy season generally occurs during the cooler months, spanning from late autumn (approximately November) to early spring (approximately April), associated mainly with Mediterranean and Red Sea trough systems. Summer precipitation, potentially linked to monsoon incursions, can occur sporadically, especially in the southern coastal areas, but is highly variable and contributes less significantly to the annual total in most parts of the region. Consequently, extended dry periods lasting several months are a common feature of the regional climate.

### 3. DATA

Daily precipitation data from eight meteorological stations in Southeast Iran for 38 years (1985–2022) was obtained from the Iran Meteorological Organization to investigate the temporal-spatial changes and statistical characteristics of extreme dry spells in Southeast Iran. This data was high quality and had minimal missing data. The missing data was reconstructed using the correlation coefficient and classic linear regression method. Data homogeneity was also checked using four types of homogeneity tests provided by Wijngaard et al. (2003): the standard normal homogeneity test, the Buishand range test, the Pettitt test, and the Von Neumann ratio test. The results of all four tests showed that the daily precipitation data of all eight studied stations in Southeast Iran are homogeneous. Figure 2 shows the names and locations of the studied stations, and Table 1 shows their geographical features in Southeast Iran.

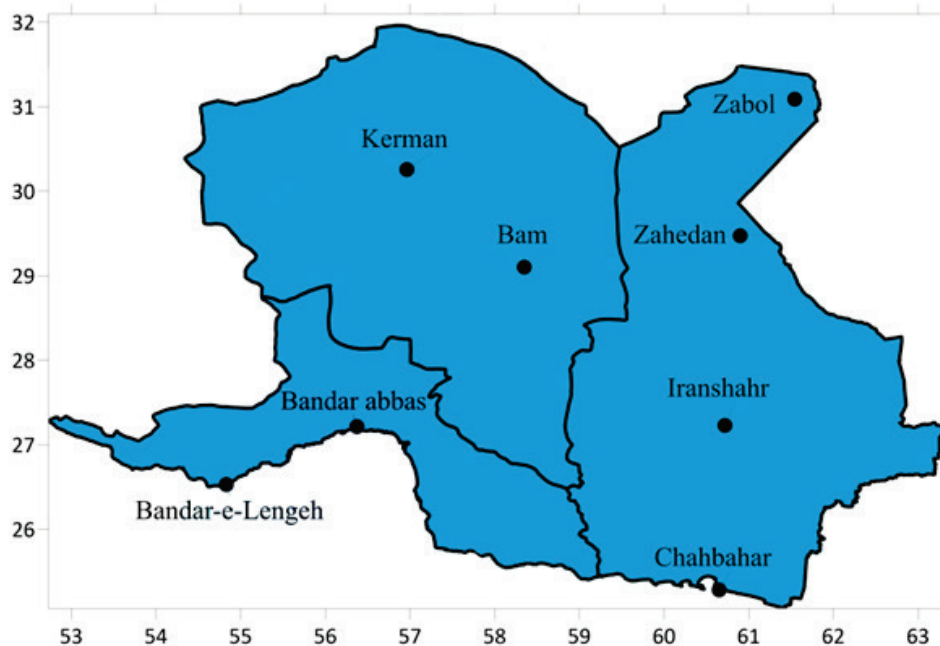


Figure 2 Distribution and dispersion of the studied stations.

Table 1 Geographical characteristics of the stations studied.

Station	Longitude	Latitude	Altitude (m)	Climate
Zahedan	60° 53′	29° 28′	1370	dry
Bam	58° 21′	29° 06′	1066.9	dry
Bandar Abbas	56° 22′	27° 13′	10	dry
Bandar Lengeh	54° 50′	26° 35′	14.2	dry
Chabahar	60° 37′	25° 17′	8	dry
Iranshar	60° 42′	27° 12′	591.1	dry
Kerman	56° 58′	30° 15′	1753.8	dry
Zabol	61° 29′	31° 02′	489.2	dry

## 4. METHODOLOGY

After collecting the data and forming the database, determining a threshold to separate more wet days from dry days looks essential. There are many differences of opinion among climatologists regarding the determination of this threshold, so they suggested various criteria such as 0.01, 0.1, 0.15, 0.2, 0.25, and 0.3 mm per day for this purpose (Alijani et al. 2015). The World Meteorological Organization (WMO) also defines a wet day with at least 1 mm of precipitation in 24 hours (Alijani et al. 2015; Domroes and Ranatunge 1993). Therefore, due to the environmental conditions of Southeast Iran and the low number of precipitation days throughout the year, this research chose the threshold of 1 mm of precipitation in one day and night, which is also approved by the WMO. Therefore, a dry spell is defined as a sequence of consecutive days with precipitation less than 1 mm per day. For each calendar year (January 1st to December 31st) within the study period (1985–2022), the LADS was identified. If a dry spell spanned across two calendar years, its total duration was calculated, and this maximum length was assigned to the calendar year in which the spell started. This approach ensures that the single longest uninterrupted dry spell associated with each year’s rainfall cycle is captured, even if it exceeds 365 days due to spanning across the year boundary.

### 4.1 Trend analysis

To investigate long-term changes in the LADS time series for each station, the non-parametric Sen’s slope estimator method (Sen 1968; Theil 1950) was employed. This method calculates the median slope across all pairs of data points in the time series, providing a robust estimate of the trend magnitude. The statistical significance of the identified trend was assessed at the 95% confidence level, typically using procedures related to the Mann-Kendall test (Gilbert 1987). A positive slope indicates an increasing trend (longer LADS over time), while a negative slope indicates a decreasing trend.

## 4.2 Probability distribution fitting and evaluation

To model the probabilistic behavior of LADS and estimate return periods, five commonly used probability distributions in hydroclimatological extreme value analysis were considered: Generalized Extreme Value (GEV), Generalized Pareto (GP), Pearson Type III (PE3), 3-parameter Lognormal (Lnorm3), and Generalized Logistic (Glogis) (Coles 2001; Rusticucci and Tencer 2008; Schubert et al. 2008; Früh et al. 2010; Weiss 1955). The parameters for each distribution were estimated using the method of L-moments (IPCC 2014; Hosking and Wallis 1997; Ghosh et al. 2016). Notably, the Generalized Logistic distribution requires a specific formulation to handle data series that include zero values, which is common in hydroclimatological data like daily precipitation. For this purpose, additional terms are defined:  $F_0$  represents the probability of a zero value, estimated as the proportion of zeros in the sample;  $b'_0$  and  $b'_1$  are the first two probability-weighted moments (PWMs) calculated exclusively from the non-zero values; and  $B_x(p, q)$  denotes the incomplete beta function. The full set of estimators for all five distributions, including the L-moments (i.e.,  $l_1, l_2, l_3, l_4$ ) and the specific parameters for the Glogis model, are detailed in Table 2.

Table 2 Cumulative distribution functions (CDF) of the five probability distributions used in this research along with  $L$  moments estimators.

Probability distribution name	Cumulative distribution functions (CDF)	Estimator of parameters
Generalized Extreme Value (GEV)	$F(x) = e^{-e^{-y}}$ <p>Where:</p> $y = \begin{cases} -k^{-1} \ln \left[ 1 - \frac{k(x - \xi)}{\alpha} \right] & k \neq 0 \\ \frac{x - \xi}{\alpha} & k = 0 \end{cases}$	$\hat{k} \approx 7.8590z + 2.9554z^2$ <p>Where:</p> $z = \frac{2}{\left[ (3 + t_3) - \left( \frac{\ln(2)}{\ln(3)} \right) \right]}$ $\hat{\alpha} = l_2 \hat{k} / \left[ (1 - 2^{-\hat{k}}) \Gamma(1 + \hat{k}) \right]$ $\hat{\xi} = l_1 - \frac{\hat{\alpha} [1 - \Gamma(1 + \hat{k})]}{\hat{k}}$
Generalized Pareto (GP)	$F(x) = 1 - e^{-y}$ <p>Where:</p> $y = \begin{cases} -k^{-1} \ln \left[ 1 - \frac{k(x - \xi)}{\alpha} \right] & k \neq 0 \\ \frac{x - \xi}{\alpha} & k = 0 \end{cases}$	$\hat{k} = \frac{(1 - 3t_3)}{(1 + t_3)}$ $\hat{\alpha} = (1 + \hat{k})(2 + \hat{k})l_2$ $\hat{\xi} = l_1 - (2 + \hat{k})l_2$
Pearson Type III (PE3)	$F(x) = \frac{1}{\beta^\alpha \int_{\xi}^x (x - \xi)^{\alpha-1} e^{-\frac{x-\xi}{\beta}} dx}$	<p>if <math>0 &lt;  t_3 </math>, then <math>z = 3\pi t_3^2</math></p> $\hat{\alpha} \approx \frac{1 + 0.2906z}{z + 0.1882z^2 + 0.0442z^3}$ <p>if <math>\frac{1}{3} \leq  t_3  &lt; 1</math> then <math>z = 1 -  t_3 </math></p> $\hat{\alpha} \approx \frac{0.36067z - 0.59567z^2 + 0.25361z^3}{1 - 2.78861z + 2.5609z^2 - 0.77045z^3}$ $\hat{\beta} = \frac{\sqrt{\pi} l_2 \Gamma(\hat{\alpha})}{\Gamma\left(\hat{\alpha} + \frac{1}{2}\right)}$ $\hat{\xi} = l_1 - \hat{\alpha} \hat{\beta}$

3-parameter Lognormal (Lnorm3)	$F(x) = \int_0^x \frac{1}{(t - \gamma)\sigma\sqrt{2\pi}} \exp\left[\frac{-1}{2\sigma^2} (\ln(t - \gamma) - \xi)^2\right] dt$ <p>Where:  <math>\hat{\gamma} = \hat{\theta}</math> and <math>\hat{\xi} = \hat{\mu}</math></p>	$\hat{\sigma}^2 = \ln \left[ \sqrt[3]{1 + \frac{1}{2}b_1^2 + \sqrt{\left(1 + \frac{1}{2}b_1^2\right)^2 - 1}} + \sqrt[3]{1 + \frac{1}{2}b_1^2 - \sqrt{\left(1 + \frac{1}{2}b_1^2\right)^2 - 1}} \right]$
		<p>Log-mean (<math>\hat{\mu}</math>):</p> $\hat{\mu} = \frac{1}{2} \ln \frac{m_2}{e^{\hat{\sigma}^2}(e^{\hat{\sigma}^2} - 1)}$
		<p>Location (<math>\hat{\theta}</math>):</p> $\hat{\theta} = \bar{x} - e^{\hat{\mu}} + \frac{\hat{\sigma}^2}{2}$
Generalized Logistic (Glogis)	$F(x) = \left[ 1 + \left[ 1 - k \left( \frac{x - \xi}{\alpha} \right)^{1/k} \right]^{-1} \right]$	$\hat{k} = -t_3$ $\hat{\alpha} = \frac{-\hat{k} \left( \frac{2b'_0}{1-F_0^2} - \frac{b'_0}{1-F_0} \right)}{\frac{2B_{1-F_0}(1+k, 2-k)}{1-F_0^2} - \frac{B_{1-F_0}(1+k, 1-k)}{1-F_0}}$ $\hat{\xi} = \frac{b'_0}{1-F_0} + \frac{\hat{\alpha}}{\hat{k}} \times \left( \frac{B_{1-F_0}(1 + \hat{k}, 1 - \hat{k})}{1 - F_0} - 1 \right)$

The suitability of each fitted distribution for describing the empirical LADS data at each station was evaluated using goodness-of-fit (GOF) tests. Specifically, the Kolmogorov-Smirnov (K-S) (Chakravarti et al. 1967) and Anderson-Darling (A-D) (Stephens 1974) tests were applied at a significance level of  $\alpha = 0.05$ . These tests compare the empirical cumulative distribution function (ECDF) derived from the observed LADS data with the theoretical cumulative distribution function (CDF) of the fitted model. The A-D test gives more weight to discrepancies in the tails of the distribution, which is often important when analyzing extremes. The distribution that passed these tests and/or demonstrated the best fit based on the test statistics was selected as the most appropriate model for subsequent return period analysis for that station or region. The specific results of the GOF tests and the selection of the best-fit distribution are presented in Section 5.

### 4.3 L-moments method

The L-moments method proposed by Hosking (1990), based on the probability-weighted method, is used to estimate the parameters of five probability distribution functions: Generalized Extreme Value (GEV), Generalized Pareto (GP) distribution, Pearson Type III (PE3) distribution, the 3-parameter Lognormal (Lnorm3) distribution, and Generalized Logistic (Glogis) distribution. The details of this method are given below.

If  $x_{1,n} \leq x_{2,n} \leq \dots \leq x_{n,n}$  are the order statistics of a considered series  $x_1, x_2, \dots, x_n$ , then the first four-order L-moments can be calculated using Equation 1:

$$\begin{cases} l_1 = b_0 \\ l_2 = 2b_1 - b_0 \\ l_3 = 6b_2 - 6b_1 + b_0 \\ l_4 = 20b_3 - 30b_2 + 12b_1 - b_0 \end{cases} \quad (1)$$

Where:

$$\begin{aligned} b_0 &= \frac{1}{n} \sum_{j=1}^n x_{j,n} \\ b_1 &= \frac{1}{n} \sum_{j=2}^n \frac{j-1}{n-1} x_{j,n} \\ b_2 &= \frac{1}{n} \sum_{j=3}^n \frac{(j-1)(j-2)}{(n-1)(n-2)} x_{j,n}, \text{ and} \\ b_3 &= \frac{1}{n} \sum_{j=4}^n \frac{(j-1)(j-2)(j-3)}{(n-1)(n-2)(n-3)} x_{j,n}. \end{aligned}$$

Next, using Equation 2, the L-moment ratios—coefficient of variation ( $t_2$ ), L-skewness ( $t_3$ ), and L-kurtosis ( $t_4$ )—are calculated as:

$$t_2 = l_2/l_1, t_3 = l_3/l_2, t_4 = l_4/l_2 \quad (2)$$

These sample L-moments and the resulting estimated parameters for the five distributions are given in Table 2.

#### 4.4 Return period estimation for LADS

After identifying the best-fit probability distribution for the LADS series at each station, we can estimate the magnitude of extreme dry spells ( $X_T$ ) which are expected to be equaled or exceeded on average once every  $T$  years (the return period). This value, ( $X_T$ ) corresponds to the quantile of the fitted distribution associated with the non-exceedance probability  $F(X_T) = 1 - T$ .

For some distributions, the quantile function (the inverse of the CDF,  $F^{-1}$ ) has an explicit analytical (closed-form) solution. Based on the relationships documented in the hydrological frequency analysis literature (She et al. 2013), the quantile functions for the GEV, GP, and Glogis distributions used in this study are:

$$GEV: X_T = \hat{\xi} + \frac{\hat{\alpha}}{\hat{k}} (1 - (-\ln(1 - 1/T))^{\hat{k}}) \quad (3)$$

$$GP: X_T = \hat{\xi} + \frac{\hat{\alpha}}{\hat{k}} (1 - (1/T)^{\hat{k}}) \quad (4)$$

$$Glogis: X_T = \hat{\xi} - \hat{\alpha} \ln \left( \left( \frac{1}{T} \right)^{\hat{k}} - 1 \right) \quad (5)$$

In these equations,  $\hat{\xi}$ ,  $\hat{\alpha}$ , and  $\hat{k}$  represent the location, scale, and shape parameters of the respective distributions estimated from the LADS data, and  $T$  is the return period in years.

Conversely, the Pearson Type 3 (PE3) and Log-Normal 3 (Lnorm3) distributions do not possess closed-form analytical solutions for their quantile functions ( $F^{-1}$ ). Therefore, estimating the LADS magnitude ( $X_T$ ) for a given return period  $T$  using these distributions requires numerical methods. In this study, the quantiles for stations where PE3 or Lnorm3 provided the best fit were computed numerically using established statistical functions available within the R software environment.

## 5. RESULTS

### 5.1 Descriptive statistics of the longest dry spells of the studied stations

The LADS for each year was extracted for all studied stations, based on the definition of dry spells. Bandar Lengeh, Chabahar, and Zabol stations have the highest averages with 211, 208, and 206 days, respectively, and Iranshahr, Kerman, and Bam stations had the lowest average of LADS with 150, 154, and 175 days (Table 3). The longest and shortest recorded LADS were recorded at Chabahar station, with 429 days (between 2001–2002), and Zabol station, with 15 days (in 1993) (Table 3). The LADS recorded for Chabahar (429 days) spanned across the calendar years of 2001 and 2002, reflecting a severe and prolonged failure of the typical rainy season during that period. The value represents the total consecutive duration of the spell assigned to the year 2001, based on our LADS identification method.

Table 3 Descriptive characteristics of the longest extreme dry spells in Southeast Iran for 1985–2022.

Station	Minimum length of dry spell (days)	Average length of dry spell (days)	Maximum length of dry spell (days)	Coefficient of variation
Zahedan	28	185	331	44.07
Bam	26	175	334	42.95
Bandar Abbas	20	184	341	39.75
Bandar Lengeh	23	211	356	42.26
Chabahar	21	208	429	47.29
Iranshahr	45	150	351	46.01
Kerman	21	154	268	36.91
Zabol	15	206	338	41

The spatial distribution of the long-term average of the LADS in Southeast Iran is illustrated in Figure 3(a). Based on this figure, the longest average extreme dry spells are observed in the coastal strip of the Oman Sea-Persian Gulf, and in the north of Sistan and Baluchestan Province (Sistan Plain). The shortest average of the LADS belonged to the center of the studied area, with a northwest-southeast direction (Figure 3a).

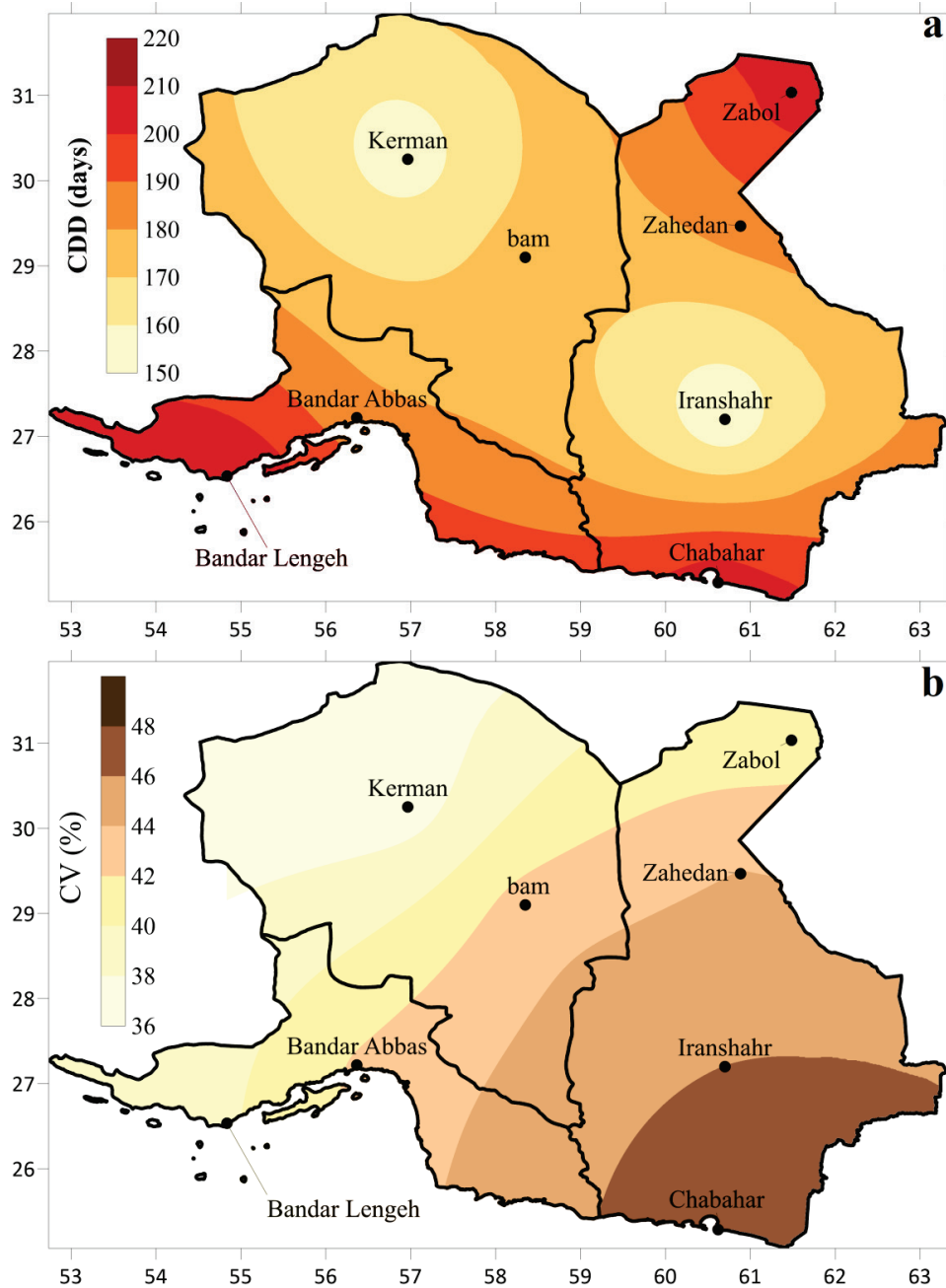


Figure 3 (a) Long-term average, and (b) Coefficient of variation of the longest extreme dry spells of Southeast Iran for the period of 1985–2022.

The coefficient of variation of the longest annual extreme dry spells of the studied stations also shows a small range of variation. Chabahar (47.29) and Iranshahr (46.01) stations have the highest coefficient of variation, and Kerman (36.91) and Bandarlange (39.75) stations have the lowest coefficient of variation values (Table 3). The coefficient of variation is an index that considers the changes of the studied variable, which are the longest annual extreme dry spells of the stations compared to their long-term average in terms of percentage. The stations whose coefficient of variation values are higher (lower) compared to other stations are stations whose longest annual extreme dry spells have high (low) changes compared to the long-term average

from year to year. Figure 3(b) shows the spatial distribution of the coefficient of variation of Southeast Iran's longest annual extreme dry spells. As observed in Figure 3(b), the coefficient of variation of the longest annual extreme dry spells from the northwest to the southeast has a clear increasing slope. In other words, the lowest coefficients of variation values are observed in the northwest and the highest are in the southeast of the study area (Figure 3b).

## 5.2 Temporal trends of LADS

The long-term trend analysis of the LADS time series for the studied stations was conducted using the non-parametric Sen's slope estimator. The results, presented in Table 4, indicate that most stations (5 out of 8, or 62.5%) exhibited an increasing trend (positive slope) in LADS during the 1985–2022 period, while the remaining 3 stations (37.5%) showed a decreasing trend (negative slope). The spatial distribution of these trends, depicted in Figure 4, does not reveal a distinct regional pattern, with stations showing increasing or decreasing trends scattered across Southeast Iran.

Table 4 Slope of the long-term change trend of the longest extreme dry spells of the studied stations, including their significance level.

Station	Trend slope (days per year)	Significant at the 95% probability level
Zahedan	0.25	0.821
Bam	0.419	0.66
Bandar Abbas	0.577	0.66
Bandar Lengeh	-0.182	0.93
Chabahar	1.085	0.565
Iranshar	-0.385	0.725
Kerman	0.143	0.92
Zabol	-0.824	0.372

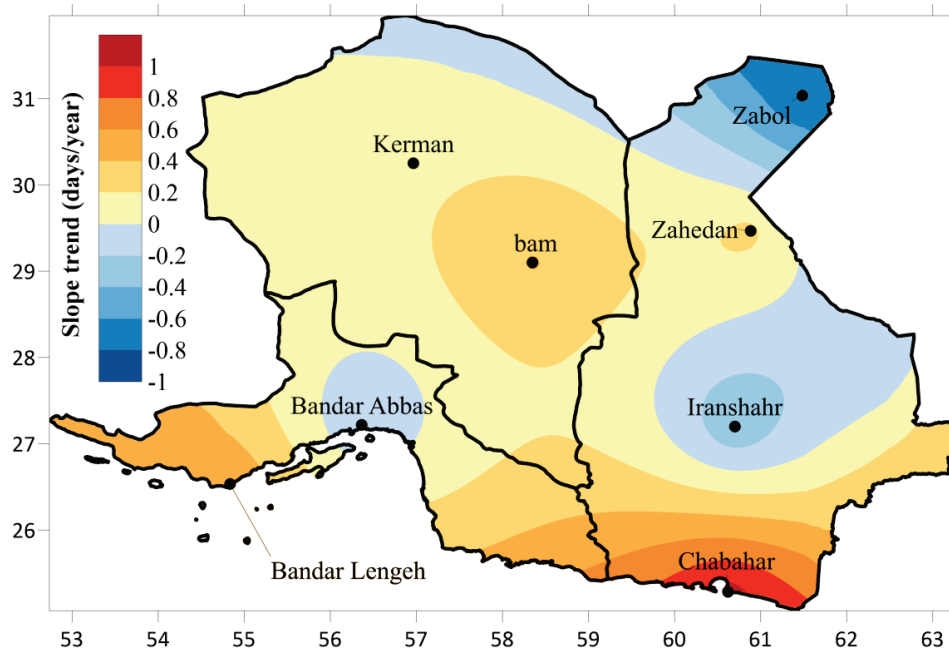


Figure 4 Spatial distribution of the slope of the long-term change trend of the LADS of the studied stations in Southeast Iran (1985–2022) in days per year.

The magnitude of the estimated trend slope ( $B$ ) varied considerably among stations. The most pronounced (though statistically non-significant) increasing trend was observed at Chabahar ( $B = 1.085$  days/year), followed by Bandar Abbas ( $B = 0.577$  days/year) and Bam ( $B = 0.419$  days/year). Conversely, the strongest decreasing trend was found at Zabol ( $B = -0.824$  days/year), followed by Iranshahr ( $B = -0.385$  days/year) and Bandar Lengeh ( $B = -0.182$  days/year) (Table 4). Importantly, none of the observed trends, whether increasing or decreasing, were statistically significant at the conventional 95% confidence level (all  $p$ -values  $> 0.05$ , see Table 4). This suggests that while there might be tendencies towards longer or shorter extreme dry spells at individual locations, these changes do not represent statistically robust long-term shifts over the study period for this region based on Sen's slope analysis. Figure 5 provides a visual representation of the LADS time series and the calculated linear trend line for each station.

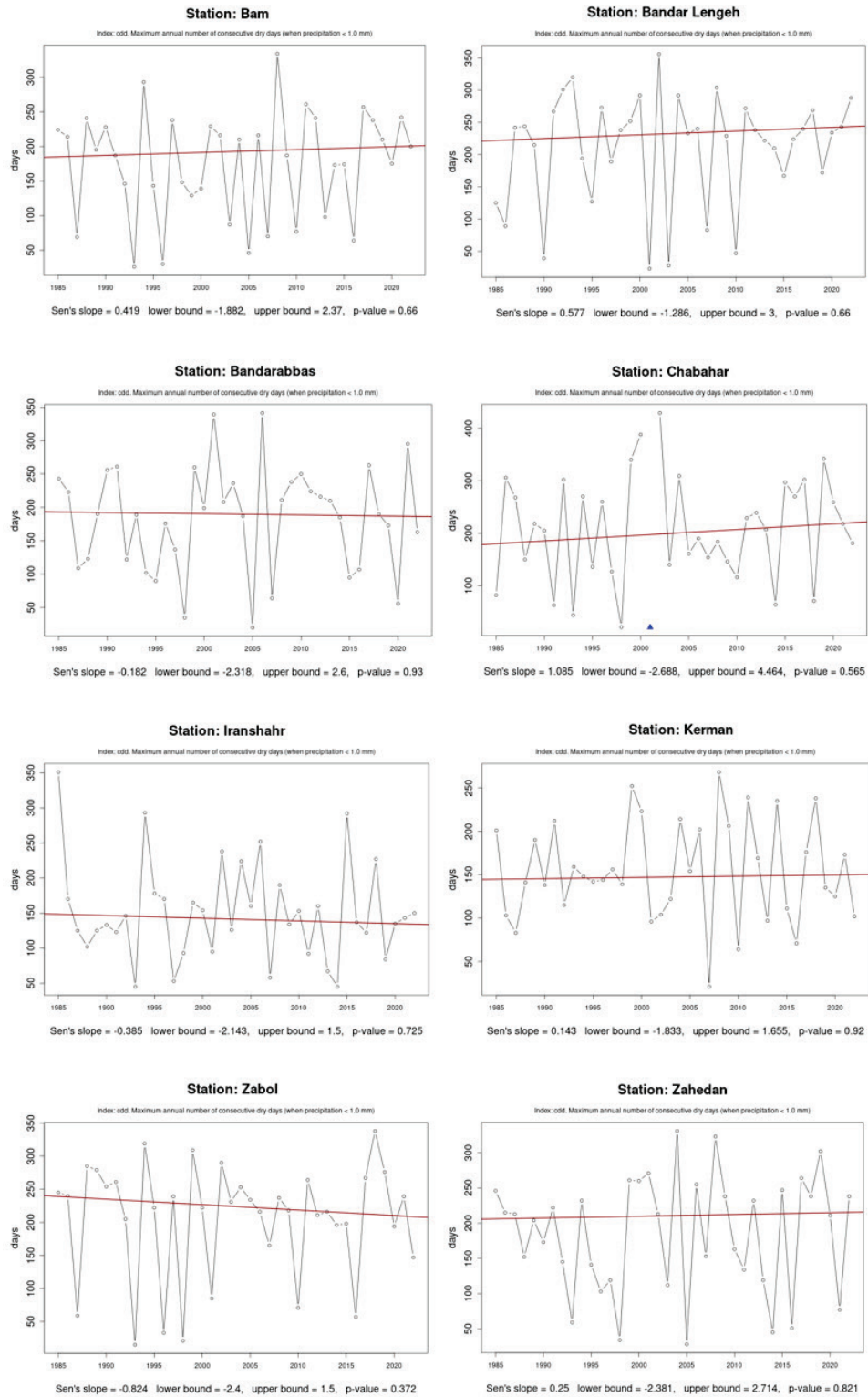


Figure 5 Slope trend of long-term changes of the LADS of the studied stations in Southeast Iran (1985–2022).

### 5.3 Frequency analysis of the LADS

To perform the frequency analysis of the LADS, five widely used probability distributions in hydro-climatological studies—Generalized Extreme Value (GEV), Generalized Pareto (GP), Pearson Type III (PE3), 3-parameter Lognormal (Lnorm3), and Generalized Logistic (Glogis)—were fitted to the LADS time series for all studied stations. The Kolmogorov-Smirnov (K-S) goodness-of-fit test was employed at a 5% significance level ( $\alpha = 0.05$ ) to identify the most suitable distribution for the LADS data at each station. The K-S test statistic ( $D_{max}$ ), representing the maximum absolute difference between the empirical and theoretical cumulative distribution functions, was calculated for each distribution and station. The distribution yielding the minimum K-S statistic is considered the best-fit, indicating the closest agreement with the observed data.

The K-S test  $p$ -values are presented in Table 5. The results indicate that the PE3 distribution provided the best fit (highest  $p$ -value) for most of the stations: Bam (0.9528), Bandar Abbas (0.9692), Bandar Lengeh (0.7020), Chabahar (0.9240), Iranshahr (0.9024), and Zabol (0.9347). The Lnorm3 distribution yielded the best fit for Kerman (0.9142), while the Glogis distribution performed best for Zahedan (0.8841). All tested distributions passed the K-S test at a 5% significance level for all stations.

Table 5 Comparison of probability values related to fitting different models to the data of meteorological stations in the center and southeast of Iran.

Station	GEV	GP	PE3	Lnorm3	Glogis	Best model
Zahedan	0.4245	0.1621	0.8362	0.3457	0.8841	Glogis
Bam	0.7234	0.1422	0.9528	0.7059	0.4271	PE3
Bandar Abbas	0.1415	0.2265	0.9692	0.1477	0.0621	PE3
Bandar Lengeh	0.2731	0.1141	0.7020	0.1955	0.0520	PE3
Chabahar	0.0929	0.1712	0.9240	0.0549	0.5622	PE3
Iranshar	0.2214	0.1425	0.9024	0.1352	0.2854	PE3
Kerman	0.1236	0.0041	0.0524	0.9142	0.3214	Lnorm3
Zabol	0.8147	0.0258	0.9347	0.2845	0.4254	PE3

NOTE: GEV: Generalized Extreme Value distribution, GP: Generalized Pareto distribution, PE3: Pearson Type III distribution, Lnorm3: 3-parameter Lognormal distribution, and Glogis: Generalized Logistic distribution.

Given that the PE3 distribution demonstrated the best fit for most stations (six out of eight) and passed the goodness-of-fit test for all locations, it was selected as the most representative regional distribution for Southeast Iran. This unified approach facilitates consistent estimation and comparison of LADS return periods (presented in Section 5.4 and Table 7) across the diverse climatic conditions within the study region.

Finally, the parameters related to the selected probability distributions of each studied station in Southeast Iran were estimated using the L-moments method. The values of the estimated parameters related to each of the selected probability distributions are given in Table 6. The parameters of the probability distributions, especially extreme-value ones, can provide useful information for characterizing severe dry-spell events.

For the PE3 distribution, the location parameter ( $\hat{\epsilon}$ , location) defines the center of the distribution, the scale parameter ( $\hat{\alpha}$ , scale) controls the spread, and the shape parameter ( $\hat{k}$ , shape) determines the skewness and overall form of the curve. For the Glogis distribution (Zahedan), the three parameters follow the same notation—location ( $\hat{\epsilon}$ ), scale ( $\hat{\alpha}$ ), and shape ( $\hat{k}$ )—but their numerical ranges and influence differ due to the logistic formulation. In contrast, the Lnorm3 distribution (Kerman) is parameterized by the mean, standard deviation ( $Sd$ ), and threshold, which have distinct interpretations in the log-normal framework. Having these parameters, the probability density functions (PDFs) and cumulative distribution functions (CDFs) for all stations can be computed. Figure 6 shows the PDFs and CDFs of three stations: Bam, Zabol, and Bandar Abbas.

Table 6 Estimated parameters of selected probability distributions using the L-moments method for the studied stations in Southeast Iran.

Station	Location ( $\hat{\epsilon}$ )	Scale ( $\hat{\alpha}$ )	Shape ( $\hat{k}$ )	Selected probability distributions
Zahedan	82.8240	-11.5210	22.8540	Glogis
Bam	31.3250	3.5874	3.2041	PE3
Bandar abbas	794.5840	3.9695	245.4700	PE3
Bandar Lengeh	66.4352	-18.8240	7.4251	PE3
Chabahar	86.8541	44.5240	2.8547	PE3
Iranshar	62.8541	60.521	1.3214	PE3
Kerman	215.0000	0.4850	0.2450	Lnorm3
Zabol	58.2000	3.4500	2.9500	PE3

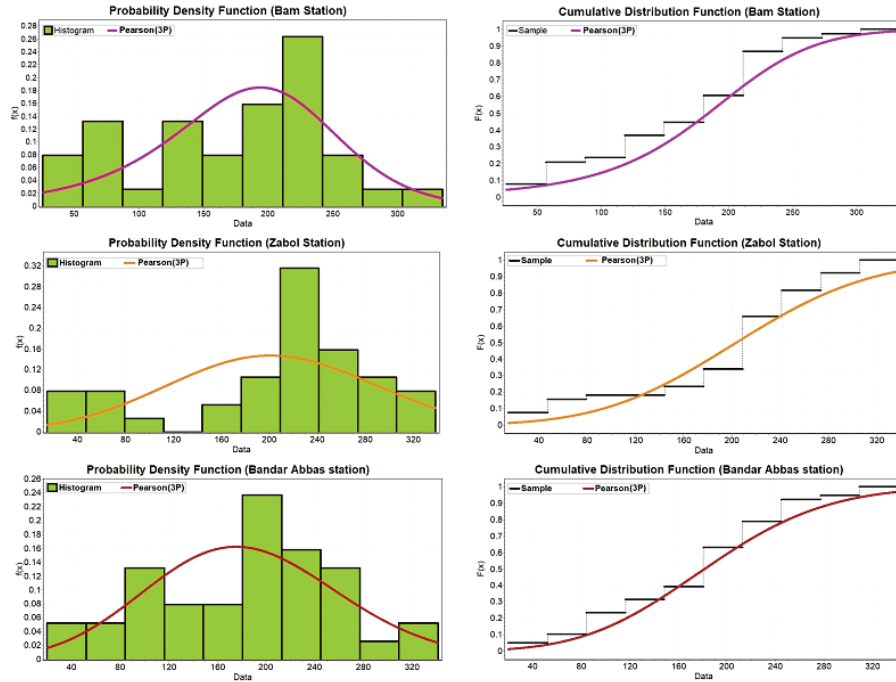


Figure 6 Probability Density Function (PDF) and Cumulative Frequency Function (CDF) of Bam, Zabol, and Bandar Abbas stations.

## 5.4 Return period of the LADS

After determining the most appropriate probability distribution fitted to the time series of the extreme dry spells of the studied stations, the return periods of 2, 5, 10, 25, 50, and 100 years were calculated. The results of these calculations are given in Table 7. As can be observed in Table 7, the LADS with a return period of 2 years are in Zabol (159.32 days), Zahedan (85.34 days), and Iranshahr (43.40 days) stations, respectively, and the shortest extreme dry spells are in Bam (22.31 days), Kerman (23.43 days), and Bandar Abbas (27.32 days) stations, respectively. Figure 7(a) shows the spatial distribution map of the extreme dry spells with a return period of 2 years. This map shows a clear southwest-to-northeast gradient for the extreme dry spells with a return period of 2 years.

Table 7 Length of extreme dry spells (days) compared with return periods (years).

Station	Return period (years)					
	2	5	10	25	50	100
Bam	22.31	66.45	114.43	163.43	210.32	255.41
Bandar Abbas	27.32	85.44	138.41	192.45	246.48	301.31
Bandar Lengeh	30.24	82.42	133.54	185.55	235.43	287.34
Chabahar	33.52	95.34	155.38	215.58	275.54	346.34
Iranshahr	43.40	108.42	176.67	238.43	306.46	372.34
Kerman	23.43	67.56	112.54	159.31	206.12	249.23
Zabol	159.32	173.34	185.23	203.43	226.65	367.48
Zahedan	85.33	118.45	149.32	184.32	218.32	249.37

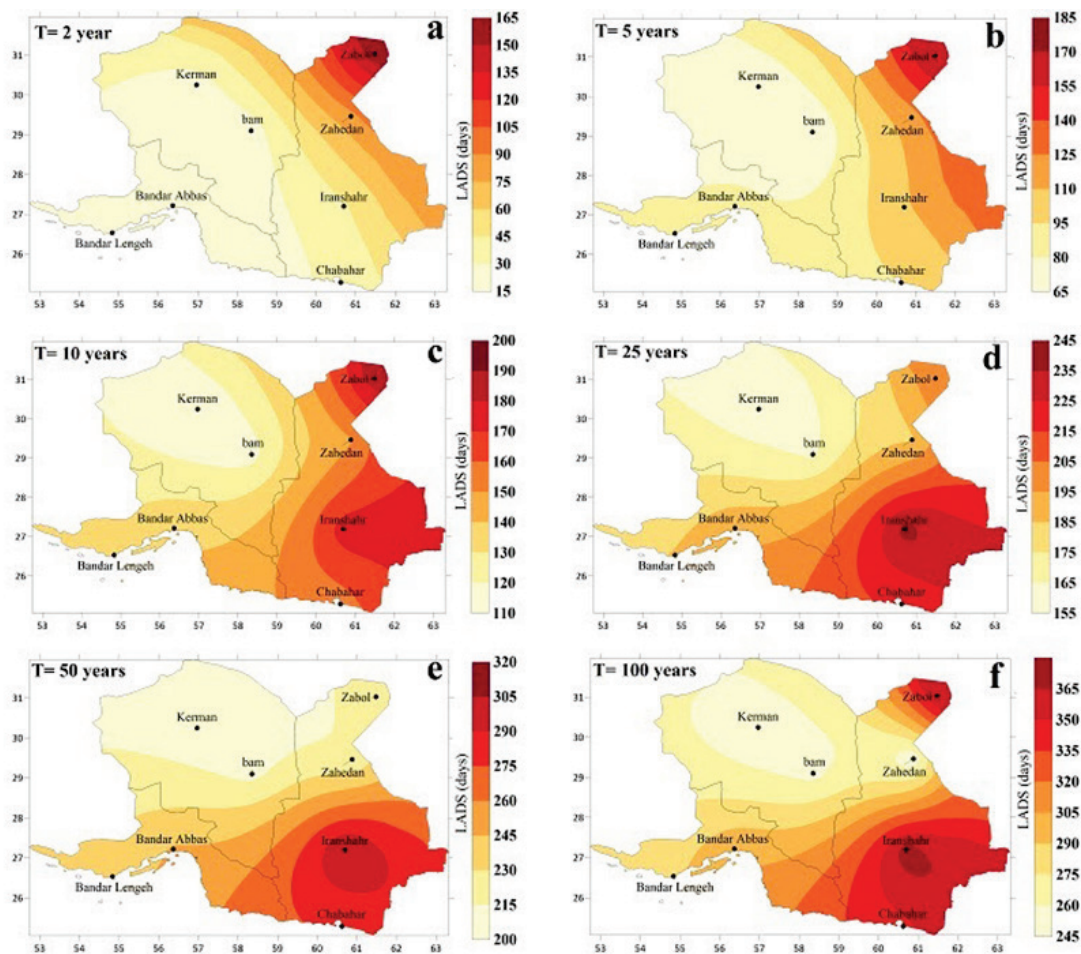


Figure 7 Spatial distribution map of extreme dry spells in Southeast Iran with return period of: (a) 2 years, (b) 5 years, (c) 10 years, (d) 25 years, (e) 50 years, and (f) 100 years.

Extreme dry spells with a return period of 5 years show that the stations located in Sistan and Baluchestan provinces have the longest extreme dry spells (Zabol station with 173.34 days, Zahedan station with 118.45 days, and Iranshahr station with 108.42 days). The stations located

in Kerman province have the shortest extreme dry spells (Bam station with 66.45 days and Kerman station with 67.56 days) (Table 7). The spatial distribution map of extreme dry spells with a 5-year return period also shows a distinct west-to-east gradient in Southeast Iran (Figure 7b).

Extreme dry spells with a return period of 10 years were also calculated for all studied stations (Table 7). Table 7 shows that the length of extreme dry spells for all stations is more than 110 days. The longest extreme dry spell for Kerman station with a return period of 10 years is 112.54 days, and is higher for Zabol station, at 185.23 days. The spatial arrangement of extreme dry spells with a 10-year return period is almost the same as that of extreme dry spells with a 5-year return period and has a west-to-east gradient (Figure 7c).

For all stations in Southeast Iran, the estimated length of extreme dry spells corresponding to a 25-year return period exceeds 160 days (Table 7). A return period of 25 years indicates that in any given year, there is a 4% chance of observing an extreme dry spell of 160 days or longer. The longest events estimated for a 25-year return period occur at Iranshahr (238.43 days) and Chabahar (215.58 days). Compared to the 2-, 5-, and 10-year return period maps, the spatial pattern at 25 years is notably different: the nucleus of the longest extreme dry spells shifts from Zabol in eastern Iran to Iranshahr in the central part of Sistan and Baluchestan Province. This shift also alters the gradient of extreme-dry-spell values, producing a northwest-to-southeast orientation (Figure 7d).

For all studied stations in Southeast Iran, the estimated duration of extreme dry spells corresponding to a 50-year return period exceeds 200 days (Table 7). A 50-year return period indicates that, in any given year, there is a 2% chance of observing an extreme dry spell of 200 days or longer. The longest such events are estimated at Iranshahr (306.46 days) and Chabahar (275.54 days) in the southern part of Sistan and Baluchestan Province. The spatial pattern for the 50-year return period is similar to that for 25 years, with the nucleus of extreme values centered over Iranshahr, and a northwest-to-southeast gradient in the length (Figure 7e).

Finally, the extreme dry spells with a return period of 100 years were calculated for all the studied stations in Southeast Iran. The results show that the extreme dry spells with a return period of 100 years for the four stations of Iranshahr (372.34 days), Zabol (367.48 days), Chabahar (346.34 days), and Bandar Abbas (301.31 days) are higher than 300 days. The extreme dry spells of other stations, including Kerman (249.23 days), Zahedan (249.37 days), Bam (255.41 days), and Bandarlang (287.34 days), have return periods between 250 and 300 days (Table 7). The same northwest-southeast gradient that existed for the 25- and 50-year return period is also observed in the spatial distribution map of the longest extreme dry spells with a 100-year return period (Figure 7f).

## 6. DISCUSSION

This study provides the first comprehensive analysis focused specifically on the stochastic modeling of the LADS using daily precipitation data across Southeast Iran, a region characterized by its arid climate and high vulnerability to drought impacts (Madani et al. 2016; Balouchi et al. 2022). By employing a standard definition of dry spells (consecutive days with < 1 mm precipitation) and analyzing a 38-year dataset (1985–2022), the study aimed to characterize the temporal trends, spatial patterns, and return periods associated with extreme dry spell events.

The analysis, using the non-parametric Sen's slope estimator, revealed a tendency towards increasing LADS duration at most stations, although these trends were generally not statistically significant at the 95% confidence level. This finding of a non-significant increasing trend contrasts with some studies in other regions, such as Catalonia, Spain, where Serra et al. (2006) found decreasing trends in dry spell characteristics based on higher thresholds (5 and 10 mm), or Peninsular Malaysia where Deni et al. (2010) reported decreasing trends for longer dry spells. However, it aligns more closely with findings in Southern Switzerland (Schmidli and Frei 2005) and parts of Croatia (Cindrić et al. 2010) where increasing trends in maximum dry spell lengths were observed, particularly in certain seasons. The lack of statistical significance in our study area might be attributed to the relatively moderate record length (38 years) for trend detection in highly variable hydroclimatic series, which is typical for arid and semi-arid regions (Mahmoudi et al. 2021). It's also worth noting that Rezaei et al. (2021), using satellite data for a shorter period (1998–2019), observed generally increasing trends in winter Maximum Consecutive Dry Days (MCDDs) across Iran, including the southeast. While this study's LADS metric is annual, the underlying signal might point towards a gradual lengthening of the most extreme dry periods within the year, warranting continued monitoring with longer datasets.

The spatial analysis of LADS characteristics revealed distinct patterns. Zabol station, located in the northern Sistan Plain, exhibited the highest LADS values for shorter return periods (2, 5, and 10 years). This suggests frequent occurrences of moderately long dry spells, potentially influenced by local factors like the strong winds of Sistan (Levar winds) exacerbating dry conditions. Conversely, for longer return periods (25, 50, and 100 years), Iranshahr station in the central part of the Sistan and Baluchestan province showed the highest estimated LADS values. This indicates that while Zabol might experience long dry spells more frequently, the potential for exceptionally prolonged, rarer dry events appears greater in the central parts of the province. These findings reinforce previous studies that consistently identify Southeast Iran as a hotspot for drought and prolonged dry conditions (Mahmoudi et al. 2013; Balouchi et al. 2022; Mahmoudi et al. 2021; Rezaei et al. 2021). Mahmoudi et al. (2013) specifically noted the significantly higher average and maximum dry spell lengths in this region compared to other parts of Iran. Our study builds upon this by providing quantitative estimates of the return periods associated with these extreme events.

The frequency analysis of LADS employed L-moments for parameter estimation and the Kolmogorov-Smirnov test for goodness-of-fit, led to the selection of the Pearson Type III (PE3) distribution as the most suitable regional model. PE3 is a widely used distribution in hydrological frequency analysis, particularly for skewed data like rainfall or streamflow extremes. The application of a regional approach based on L-moments (Hosking and Wallis 1997) is advantageous in regions with limited data, as it pools information across stations to derive more robust parameter estimates.

However, a critical point raised during the review process, and a common challenge in extreme value analysis, is the comparison between the maximum observed event in the historical record (Table 3), and the estimated LADS for long return periods (e.g., 100 years, Table 7). We observed that for six stations (Bam, Bandar Abbas, Bandar Lengeh, Chabahar, Kerman, and Zahedan), the observed LADS exceeded the estimated 100-year LADS. The 429-day spell observed in Chabahar is particularly noteworthy. This apparent discrepancy warrants careful consideration.

First, it is statistically plausible for a relatively short observational record (38 years) to capture an event whose actual return period is significantly longer than the record length or the target return period being estimated (e.g., the observed 429-day event might be a 200-year or rarer event that occurred by chance during our study period). Second, while PE3 provided the best overall fit based on the K-S test, this test assesses the fit across the entire distribution range. It's possible that the PE3 model, despite its overall suitability, might slightly underestimate the probabilities in the extreme upper tail, leading to lower estimates for very rare events (e.g., 100-year return period). Uncertainties in parameter estimation, particularly for distributions with three parameters like PE3 fitted to limited data, can also contribute. Finally, extrapolating far beyond the record length (estimating 100-year events from 38 years of data) inherently involves significant uncertainty. Therefore, the results in Table 7 should be interpreted as probabilistic estimates based on the best-fitting regional model, while the values in Table 3 represent the actual, albeit potentially rare, extremes experienced during the specific observation period. Both pieces of information are valuable: the observed maximums highlight the documented severity of dry spells, while the return period estimates provide a standardized measure of risk for planning purposes.

This study, while providing novel insights, has several limitations that open avenues for future research. The 38-year data record, although the longest available consistent daily data for the selected stations, is still relatively short for robustly estimating very long return periods (e.g., 100 years) and detecting statistically significant long-term trends. The spatial coverage, limited to eight stations across a vast and geographically diverse area, could be improved by incorporating data from more stations or utilizing high-resolution gridded precipitation datasets (e.g., satellite-based like TRMM used by Rezaei et al. (2021) or reanalysis products), though these often come with their own uncertainties and shorter record lengths. The choice of a 1 mm threshold for defining a dry day is standard but somewhat arbitrary; exploring sensitivity to different thresholds could provide additional insights.

Furthermore, this study focused solely on the LADS. Future work could investigate other dry spell characteristics, such as the frequency of spells exceeding certain durations or the total number of dry days per year. A significant improvement, as suggested by the reviewer, would be to validate the return period estimates using stochastic simulation. Developing and validating a daily weather generator capable of accurately reproducing the precipitation characteristics of Southeast Iran (including the persistence of dry and wet days) would allow for the generation of very long synthetic time series (e.g., 1000+ years). Analyzing LADS from these simulations could provide an independent check on the return period estimates derived from the fitted theoretical distributions and help assess the adequacy of the PE3 model in the extreme tail. Additionally, future studies should aim to investigate the underlying drivers of LADS variability and trends, potentially linking them to large-scale climate oscillations (e.g., ENSO, the Madden-Julian Oscillation (MJO), and the Indian Ocean Dipole (IOD)) known to influence regional climate, as explored for winter MCDD by Rezaei et al. (2021), and incorporating climate change projections.

## 7. CONCLUSION

This study presented the first comprehensive stochastic analysis focused specifically on the LADS in the data-scarce and drought-vulnerable region of Southeast Iran, utilizing daily

precipitation records from eight stations spanning 38 years (1985–2022). The primary objective was to characterize the temporal trends, spatial patterns, and return periods associated with these extreme events.

The trend analysis, employing Sen’s slope estimator, revealed a tendency towards longer LADS durations at most stations during the study period. However, it is crucial to emphasize that these increasing trends generally lacked statistical significance at the 95% confidence level across the region. Therefore, while a potential shift towards longer dry spells might be occurring, the available 38-year record does not provide conclusive statistical evidence of a long-term, region-wide significant increase.

Regional frequency analysis using L-moments identified the PE3 distribution as the most suitable model for describing the probability distribution of LADS across Southeast Iran. Based on the selected PE3 model, estimates of LADS for various return periods highlighted distinct spatial patterns:

- For shorter return periods (2, 5, and 10 years), Zabol station in the northern Sistan plain exhibited the longest estimated LADS (e.g., approximately 185 days for a 10-year event).
- For longer return periods (25, 50, and 100 years), the locus of the most extreme estimated LADS shifted towards the central parts of the region, with Iranshahr station showing the highest values (e.g., approximately 372 days for a 100-year event).

Although the observed trends were statistically non-significant, the magnitude of the estimated LADS values, particularly for longer return periods (as shown in Table 7), combined with the documented instances of extremely long observed dry spells (LADS in Table 3, discussed in Section 4.3), unequivocally underscores the region’s inherent and significant vulnerability to prolonged drought conditions. These findings quantify the substantial risk posed by extreme dry spells, irrespective of the statistical significance of recent trends in the available data period.

In summary, this research provides quantitative estimates of extreme dry spell characteristics and associated return periods specific to Southeast Iran. This information is vital for informed water resource management, agricultural planning, infrastructure design (e.g., drainage systems), and drought risk assessment in one of Iran’s most hydro-climatically sensitive areas. The results emphasize the need for proactive drought preparedness strategies informed by the quantified potential for exceptionally long dry periods in the region.

## REFERENCES

- Alijani, B., P. Mahmoudi, A. Shahoozahi, and A. Mohammadi. 2015. "Study of the persistence of precipitation days in Iran." *Geography and Environmental Planning* 25 (4): 1–16 (in Persian).
- Alizadeh-Choobari, O. and M.S. Najafi. 2018. "Extreme weather events in Iran under a changing climate." *Climate Dynamics* 50: 249–260. <https://doi.org/10.1007/s00382-017-3602-4>
- Anagnostopoulou, C., P. Maheras, T. Karacostas, and M. Vafiadis. 2003. "Spatial and temporal analysis of dry spells in Greece." *Theoretical and Applied Climatology* 74 (1–2): 77–91. <https://doi.org/10.1007/s00704-002-0713-5>
- Balouchi, Z., P. Mahmoudi, and M. Hamidianpour. 2022. "Analyzing Iran's Local and Regional Droughts Using the Theory of Runs and Standardized Precipitation Index (SPI)." *Journal of Arid Regions Geographic Studies* 12 (46): 53–75 (in Persian).
- Bari Abarghouei, H., M.A. Asadi Zarch, M.T. Dastorani, M.R. Kousari, and M. Safari Zarch. 2011. "The survey of climatic drought trend in Iran." *Stochastic Environmental Research and Risk Assessment* 25, 1–14. <https://doi.org/10.1007/s00477-011-0491-7>
- Bonsal, B.R., X. Zhang, L.A. Vincent, and W.D. Hogg. 2001. "Characteristics of daily and extreme temperatures over Canada." *Journal of Climate* 14 (9): 1959–1976. [https://doi.org/10.1175/1520-0442\(2001\)014<1959:CODAET>2.0.CO;2](https://doi.org/10.1175/1520-0442(2001)014<1959:CODAET>2.0.CO;2)
- Byun, H.R. and D.A. Wilhite. 1999. "Objective quantification of drought severity and duration." *Journal of Climate* 12 (9): 2747–2756. [https://doi.org/10.1175/1520-0442\(1999\)012<2747:OQODSA>2.0.CO;2](https://doi.org/10.1175/1520-0442(1999)012<2747:OQODSA>2.0.CO;2)
- Chakravarti, I.M., R.G. Laha, and J. Roy. 1967. *Handbook Methods of Applied Statistics, Volume I*, pp. 11–27. John Wiley and Sons, New York.
- Chanda, K., R. Maity, A. Sharma, and R. Mehrotra. 2014. "Spatiotemporal variation of long-term drought propensity through reliability-resilience-vulnerability based Drought Management Index." *Water Resources Research* 50 (10): 7662–7676. <https://doi.org/10.1002/2014WR015703>
- Cindrić, K., Z. Pasarić, and M. Gajić-Čapka. 2010. "Spatial and temporal analysis of dry spells in Croatia." *Theoretical and Applied Climatology* 102: 171–184. <https://doi.org/10.1007/s00704-010-0250-6>
- Coles, S. 2001. *An Introduction to Statistical Modeling of Extreme Values*, pp. 209. Springer, London.
- De Martonne, M. 1909. "Traité de géographie physique – Climat – Hydrographie – Relief du sol – Biogéographie." Librairie Armand Colin, Paris.
- Deni, S.M., J. Suhaila. W.Z. Wan Zin, and A.A. Jemain. 2010. "Spatial trends of dry spells over Peninsular Malaysia during monsoon seasons." *Theoretical and Applied Climatology* 99, 357–371. <https://doi.org/10.1007/s00704-009-0147-4>

- Domroes, M. and E. Ranatunge. 1993. "A statistical approach toward a regionalization of daily rainfall in Sri Lanka." *International Journal of Climatology* 13 (7): 741–754. <https://doi.org/10.1002/joc.3370130704>
- Douguedroit, A. 1987. "The variations of dry spells in Marseilles from 1865 to 1984." *Journal of Climatology* 7 (6): 541–551. <https://doi.org/10.1002/joc.3370070603>
- Früh, B., H. Feldmann, H.J. Panitz, G. Schädler, D. Jacob, P. Lorenz, and K. Keuler. 2010. "Determination of precipitation return values in complex terrain and their evaluation." *Journal of Climate* 23 (9): 2257–2274. <https://doi.org/10.1175/2009JCLI2685.1>
- Ghaemi, A., S.A. Hashemi Monfared, A. Bahrpeyma, P. Mahmoudi, and M. Zounemat-Kermani. 2022. "Spatiotemporal variation of projected drought characteristics of Iran under the climate change scenarios." *Journal of Meteorology and Atmospheric Science* 5 (1): 68–80 (in Persian).
- Ghosh, S., M.K. Roy, and S.C. Biswas. 2016. "Determination of the Best Fit Probability Distribution for Monthly Rainfall Data in Bangladesh." *American Journal of Mathematics and Statistics* 6 (4): 170–174.
- Gilbert, R.O. 1987. *Statistical Methods for Environmental Pollution Monitoring*. John Wiley and Sons, New York.
- Hosking, J.R.M. 1990. "L-moments: Analysis and estimation of distributions using linear combinations of order statistics." *Journal of the Royal Statistical Society. Series B (Methodological)* 52 (1): 105–124. <https://doi.org/10.1111/j.2517-6161.1990.tb01775.x>
- Hosking, J.R.M. and J.R. Wallis. 1997. *Regional Frequency Analysis: An Approach Based on L-Moments*. Cambridge University Press, Cambridge, UK.
- IPCC. 2014. "Climate Change 2014: Synthesis Report." Contribution of Working Groups I, II and III to the Fifth Assessment Report of the Intergovernmental Panel on Climate Change [Core Writing Team, R.K. Pachauri and L.A. Meyer (eds.)], pp. 151. Geneva, Switzerland.
- Kutiél, H. 1985. "The multimodality of the rainfall course in Israel as reflected by the distribution of dry spells." *Archives for Meteorology, Geophysics, and Bioclimatology, Series B* 36, 15–27. <https://doi.org/10.1007/BF02269454>
- Madani, K., A. AghaKouchak, and A. Mirchi. 2016. "Iran's Socio-economic Drought: Challenges of a Water-Bankrupt Nation." *Iranian Studies* 49 (6): 997–1016. <https://doi.org/10.1080/00210862.2016.1259286>
- Mahmoudi, P., S.M. Amir Jahanshahi, N. Daneshmand, and J. Rezaei. 2021. "Spatial and temporal analysis of mean and frequency variations of dry spells in Iran." *Arabian Journal of Geosciences* 14, 478. <https://doi.org/10.1007/s12517-021-06861-6>
- Mahmoudi, P., M. Hamidian Pour, M. Sanaei, and N. Daneshmand. 2019. "Investigating the Trends of Drought Severity Changes in Iran." In: *Proceedings of International Conference on Climate Change, Impacts, Adaptation and Mitigation*, 11 June, Kharzmi University, Tehran, Iran.
- Mahmoudi, P., R. Maity, S.M. Amir Jahanshahi, and K. Chanda. 2022. "Changing spectral patterns of long-term drought propensity in Iran through reliability–resilience–

- vulnerability-based Drought Management Index." *International Journal of Climatology* 42 (8): 4147–4163. <https://doi.org/10.1002/joc.7454>
- Mahmoudi, P., N. Parvin, and J. Rezaei. 2013. "Regionalization of Iran based on the length of dry spells." *Arid Regions Geographic Studies* 4 (13): 85–106 (in Persian).
- Mansouri Daneshvar, M.R., M. Ebrahimi, and H. Nejadsoleymani. 2019. "An overview of climate change in Iran: Facts and statistics." *Environmental Systems Research* 8, 7. <https://doi.org/10.1186/s40068-019-0135-3>
- Martin-Vide, J. and L. Gomez. 1999. "Regionalization of Peninsular Spain based on the length of dry spells." *International Journal of Climatology* 19 (5): 537–555. [https://doi.org/10.1002/\(SICI\)1097-0088\(199904\)19:5<537::AID-JOC371>3.0.CO;2-X](https://doi.org/10.1002/(SICI)1097-0088(199904)19:5<537::AID-JOC371>3.0.CO;2-X)
- McKee, T.B., N.J. Doesken, and J. Kleist. 1993. "The relationship of drought frequency and duration to time scale." In: *Proc. of Eighth Conference on Applied Climatology*, 1993, 179–184. American Meteorological Society, Anaheim, CA.
- McKee, T.B., N.J. Doesken, and J. Kleist. 1995. "Drought monitoring with multiple time scales." In: *Proc. of Ninth Conference on Applied Climatology*, 233–236. American Meteorological Society, Dallas, TX.
- Mishra, A.K. and V.P. Singh. 2010. "A review of drought concepts." *Journal of Hydrology* 391 (1–2): 202–216. <https://doi.org/10.1016/j.jhydrol.2010.07.012>
- Nouri, M. and M. Homaee. 2020. "Drought trend, frequency and extremity across a wide range of climates over Iran." *Meteorological Applications* 27 (2): 1–19. <https://doi.org/10.1002/met.1899>
- Palmer, W.C. 1965. "Meteorological Drought." Res. Paper No. 45, 768 Weather Bureau, Washington, D.C.
- Rezaei, M., E. Rousi, E. Ghasemifar, and A. Sadeghi. 2021. "A study of dry spells in Iran based on satellite data and their relationship with ENSO." *Theoretical and Applied Climatology* 144, 1387–1405. <https://doi.org/10.1007/s00704-021-03607-y>
- Rusticucci, M. and B. Tencer. 2008. "Observed changes in return values of annual temperature extremes over Argentina." *Journal of Climate* 21: 5455–5467. <https://doi.org/10.1175/2008JCLI2190.1>
- Schmidli, J. and C. Frei. 2005. "Trends of heavy precipitation and wet and dry spells in Switzerland during the 20th century." *International Journal of Climatology* 25 (6): 753–771. <https://doi.org/10.1002/joc.1179>
- Schubert, S.D., Y. Chang, M.J. Suarez, and P.J. Pegion. 2008. "ENSO and wintertime extreme precipitation events over the contiguous United States." *Journal of Climate* 21 (1): 22–39. <https://doi.org/10.1175/2007JCLI1705.1>
- Sen, P.K. 1968. "Estimates of the Regression Coefficient Based on Kendall's Tau." *Journal of the American Statistical Association* 63 (324): 1379–1389. <https://doi.org/10.1080/01621459.1968.10480934>

- Serra, C., A. Burgueño, M. Martínez, and X. Lana. 2006. "Trends in dry spells across Catalonia (NE Spain) during the second half of the 20th century." *Theoretical and Applied Climatology* 85: 165–183. <https://doi.org/10.1007/s00704-005-0184-6>
- She, D., J. Xia, J. Song, H. Du, J. Chen, and L. Wan. 2013. "Spatio-temporal variation and statistical characteristic of extreme dry spell in Yellow River Basin, China." *Theoretical and Applied Climatology* 112, 201–213. <https://doi.org/10.1007/s00704-012-0731-x>
- Statistical Center of Iran. 2016. "Census 2016 – General Results" (in Persian). <https://amar.org.ir/population-and-migration>
- Stephens, M.A. 1974. "EDF Statistics for Goodness of Fit and Some Comparisons." *Journal of the American Statistical Association* 69, 730–737. <https://doi.org/10.2307/2286009>
- Theil, H. 1950. "A Rank-Invariant Method of Linear and Polynomial Regression Analysis." *Nederlandse Akademie Wetenschappen Series A*, 53, 3860392.
- Vicente-Serrano, S., S. Beguería, J.L. López-Moreno. 2010. "A multiscalar drought index sensitive to global warming: the standardized precipitation evapotranspiration index." *Journal of Climate* 23 (7): 1696–1718. <https://doi.org/10.1175/2009JCLI2909.1>
- Weiss, L.L. 1955. "A nomogram based on the theory of extreme values for determining values for various return periods." *Monthly Weather Review* 83: 69–71. [https://doi.org/10.1175/1520-0493\(1955\)083<0069:ANBOTT>2.0.CO;2](https://doi.org/10.1175/1520-0493(1955)083<0069:ANBOTT>2.0.CO;2)
- Wijngaard, J.B., A.M.G. Klein Tank, and G.P. Konnen. 2003. "Homogeneity of 20th century European daily temperature and precipitation series." *International Journal of Climatology* 23 (6): 679–692. <https://doi.org/10.1002/joc.906>
- Wilhite, D.A. and R.S. Pulwarty. 2017. "Drought as Hazard: Understanding the Natural and Social Context." In: D.A. Wilhite and R.S. Pulwarty (Editors), *Drought and Water Crises*, pp. 3–22. CRC Press, Boca Raton.
- Zarrin, A., D. Yazdany, and A.A. Dadashi-Roudbari. 2022. "Projection of minimum and maximum temperatures in cold regions of Iran using SDSM statistical downscaling model." *Climate Change Research* 3 (10): 19–32 (in Persian). <https://doi.org/10.30488/ccr.2022.340823.1078>